Comparative analysis of transient receptor potential channel 5 opposite strand-induced gene expression patterns and protein-protein interactions in triple-negative breast cancer

JINGHUI PENG[1,2*], SHENGBIN PEI[1,2*], YANGYANG CUI[1*], YIQIN XIA[1], YUE HUANG[1], XIAOWEI WU[2], MINGJIE ZHENG[1], MIAOMIAO WENG[1], XU HAN[1,2], HONGTAO FU[1,2], LILI YANG[1], WENBIN ZHOU[1], ZIYI FU[2], SHUI WANG[1] and HUI XIE[1]

[1]Department of Breast Surgery and [2]Breast Disease Laboratory, Women and Children Central Laboratory, The First Affiliated Hospital, Nanjing Medical University, Nanjing, Jiangsu 210029, P.R. China

Received February 8, 2021; Accepted April 4, 2022

DOI: 10.3892/ol.2022.13379

Abstract. In patients with triple-negative breast cancer (TNBC), high tumour mutation burden and aberrant oncogene expression profiles are some of the causes of poor prognosis. Therefore, it is necessary to identify aberrantly expressed oncogenes, since they have the potential to serve as therapeutic targets. Transient receptor potential channel 5 opposite strand (TRPC5OS) has been previously shown to function as a novel tumour inducer. However, the underlying mechanism of TRPC5OS function in TNBC remain to be elucidated. Therefore, in the present study TRPC5OS expression was first measured in tissue samples of patients with TNBC and a panel of breast cancer cell lines (ZR-75-1, MDA-MB-453, SK-BR-3, JIMT-1, BT474 and HCC1937) by using qRT-PCR and Western blotting. Subsequently, the possible effects of TRPC5OS on MDA-MB-231 cells proliferation were determined using Cell Counting Kit-8 and 5-Ethynyl-2'-deoxyuridine assays after Lentiviral transfection of MDA-MB-231. In addition, potential interaction partners of TRPC5OS were explored using liquid chromatography-mass spectrometry (LC-MS)/MS. Gene expression patterns following TRPC5OS overexpression were also detected in MDA-MB-231 cells by using High-throughput sequencing. Gene Ontology (GO) and Kyoto Encyclopaedia of Genes and Genomes (KEGG) analysis were then used to systematically verify the potential interactions among the TRPC5OS-regulated genes. The potential relationship between TRPC5OS-interacting proteins and gene expression patterns were studied using Search Tool for the Retrieval of Interacting Genes/Proteins (STRING) analysis. TRPC5OS expression was found to be significantly higher in TNBC tumour tissues and breast cancer cell lines compared with luminal tumour tissues and ZR-75-1. In addition, the overexpression of TRPC5OS significantly increased cell proliferation. High-throughput sequencing results revealed that 5,256 genes exhibited differential expression following TRPC5OS overexpression, including 3,269 upregulated genes and 1,987 downregulated genes. GO analysis results indicated that the functions of these differentially expressed genes were enriched in the categories of 'cell division' and 'cell proliferation' regulation. KEGG analysis showed that the TRPC5OS-regulated genes were associated with processes of 'homologous recombination' and 'TNF signalling pathways'. Subsequently, 17 TRPC5OS-interacting proteins were found using LC-MS/MS and STRING analysis. The most important protein among interacting proteins was ENO1 which was associated with glycolysis and regulated proliferation of cancer. In summary, data from the present study suggest that TRPC5OS overexpression can increase TNBC cell proliferation and ENO1 may be a potential target protein mediated by TRPC5OS. Therefore, TRPC5OS may serve as a novel therapeutic target for TNBC.

Correspondence to: Professor Shui Wang or Professor Hui Xie, Department of Breast Surgery, The First Affiliated Hospital, Nanjing Medical University, 300 Guangzhou Road, Nanjing, Jiangsu 210029, P.R. China
E-mail: shwang@njmu.edu.cn
E-mail: hxie@njmu.edu.cn

*Contributed equally

Key words: triple-negative breast cancer, transient receptor potential channels 5 opposite strand, proliferation, bioinformatics analysis

Introduction

Over the last 5 years, the incidence of breast cancer has increased by 0.3% per year (1), although the mortality rate has decreased by 40% between 1989 and 2017 in the United States (1). However, the clinical prognosis from TNBC remains poor (2). Compared with other subtypes of breast cancer, TNBC are relatively more common in younger patients, the clinical characteristics of which tend to be more aggressive (2). In addition, patients with TNBC frequently present with larger tumour masses, where lesions with higher grades are more likely to be detected (3-5). In total ~33% patients with TNBC will develop metastatic disease (6,7). The lack of

effective therapeutic strategies for TNBC, such as endocrine therapy or targeted therapy, is one of the key reasons for the poor prognosis of TNBC (8). Therefore, further exploration of novel targets for the treatment of TNBC is warranted to improve the prognosis from this disease.

Transient receptor potential channels 5 (TRPC5) has been previously reported to regulate various biological processes such as oxidative stress, constitutively active TRPs, and neuronal cell death (9). Accumulating evidence suggests that TRPC5 can serve an important role in promoting resistance to chemotherapy in breast cancer (10-12). As such, increased TRPC5 expression has been reported to induce the expression of P-glycoprotein in MCF-7 cells (12). Subsequently, P-glycoprotein then functions to remove cytotoxic drugs from the cells to mediate chemotherapy resistance (13).

TRPC5 opposite strand (OS) is the antisense strand of TRPC5 and is also known as TRPC5 antisense RNA1 (TRPC5-AS1) (14). TRPC5OS has been previously found to encode a microprotein that consists of 111 amino acids and is highly expressed particularly in the testis (15). Genes that are specifically expressed in normal testicular tissues may serve an important role in liver cancers, such as the OY-TES-1 gene. Under physiological conditions, OY-TES-1 mRNA is only expressed in the testis (13). However, its expression has been reported to be upregulated in several types of cancer, such as bladder cancer and breast cancer, where it has been shown to be a novel member of the cancer/testicular antigen family (14). In addition, the OSs of other important genes, such as long non-coding RNA FOXD2 adjacent opposite strand RNA 1 (FOXD2-AS1) and the antisense strand of HOXA11 (HOXA11-AS) may also be associated with the occurrence and development of breast cancer. There is evidence that interfering with HOXA11-AS and FOXD2-AS1 function can attenuate the invasive and migratory capabilities of breast cancer cells (16,17). Therefore, it could be hypothesised that TRPC5OS may affect the physiology of tumours by regulating tumour progression, in turn affecting patient prognosis. However, little is known regarding the possible role of TRPC5OS in breast cancer. Therefore, in the present study, the aim is to elucidate the possible function and mechanism of TRPC5OS in TNBC, to explore its potential value as a novel therapeutic target.

Materials and methods

Cell lines and culture. The human breast cancer cell lines ZR-75-1, MDA-MB-453, SK-BR-3, JIMT-1, BT474, HCC1937 and SUM-1315, in addition to the normal human breast cancer cell line MCF-10A, were gifts from Professor Ziyi Fu (Breast Disease Laboratory, Women & Children Central Laboratory, First Affiliated Hospital, Nanjing Medical University). The human breast cancer cell lines MDA-MB-231 and MCF-7 were purchased from The Cell Bank of Type Culture Collection of the Chinese Academy of Sciences (https://www.cellbank.org.cn/). MCF-10A, ZR-75-1, MDA-MB-453, SK-BR-3, JIMT-1, BT474, HCC1937, MDA-MB-231, SUM-1315 and MCF-7 cells were cultured in high-glucose DMEM (Gibco; Thermo Fisher Scientific, Inc.) supplemented with 10% (v/v) FBS (Gibco; Thermo Fisher Scientific, Inc.) 100 U/ml penicillin (Gibco; Thermo Fisher Scientific, Inc.) and 100 U/ml streptomycin (Gibco; Thermo Fisher Scientific, Inc.) in a humidified atmosphere with 5% CO_2 at 37˚C. MCF-10A cells are normal mammary epithelial cells (18), whereas BT474, MCF-7 and ZR-75-1 cells are luminal-type breast cancer cells (18). HCC1937, MDA-MB-231 and SUM-1315 are TNBC cells, whilst JIMT-1, SK-BR-3 and MDA-MB-453 are oestrogen receptor (ER)-, progesterone receptor (PR)-, human epidermal growth factor receptor 2 (HER)+ breast cancer cells (18). All experiments were independently reproduced three times.

Patient tissue samples. A total of 30 pairs of breast cancer tissues and matching adjacent normal tissues (3-5 cm from the edge of the breast cancer tissues) were obtained from Jiangsu Province Hospital (Table SI). All tissues were collected from 2015-2018 and tumour size was obtained from postoperative pathological reports. All patients were female and mean ± SD age was 53.17±11.94. Written informed consent was obtained from all patients recruited in the present study. The present study was approved by the Ethics Committee of Jiangsu Province Hospital (The First Hospital Affiliated Hospital with Nanjing Medical University; approval no. 2010-SR-091). The inclusion criteria were: i) Patients diagnosed with TNBC by immunohistochemical method after ultrasound-guided core-needle biopsy and ii) no active therapy prior to operative treatment. Patients undergoing neoadjuvant chemotherapy or with multiple neoplasm were excluded. Tissues were obtained by surgical resection and stored in a -80˚C refrigerator for utilization.

Lentiviral transfection of MDA-MB-231 and MCF-7 cells. MDA-MB-231 and MCF-7 cells were incubated in six-well plates. After confluency reached 50%, cells were transfected with 5 μg/ml LV-TRPC5OS, LV5 (NC; the overexpression control; EF-1Af/GFP&Puro), LV-193 (sh-TRPC5OS, GGG AGAATTTGTCTCTGAAGT) and LV3 (NC; the knockdown control; H1/GFP&Puro) for 6 h. The generation system used was 3rd, the temporary cell line used was 293 cells (Chinese Academy of Medical Sciences Tumor Cell Bank). MOI=-In (0.01)=4.6 pfu/cell. The ratio of the lentiviral plasmid: packaging vector: envelope=1:2:1. All agents and products were obtained from Shanghai GenePharma, Co., Ltd. In total, 3 μg/ml puromycin (VWR, Avantor, Inc.) was used to screen cells that had been successfully transfected for 2 weeks at 37˚C. Transfection efficiency was confirmed using fluorescence microscopy following screening (magnification of fluorescence microscopy was x40).

Cell Counting Kit-8 (CCK-8) assay. A total of $2x10^3$ MDA-MB-231 or MCF-7 cells in 100 μl high-glucose DMEM culture solution per well were added into a 96-well plate and incubated overnight. Subsequently, it was tested daily for ≤6 days. Prior to testing, 90 μl serum-free medium with 10 μl CCK-8 labelling reagent (Dojindo, Molecular Technologies, Inc.) was added into each well and incubated for 2 h in the dark at 37˚C. The viability of the cells was then analysed by measuring their absorbance at 450 nm using an enzyme-labelled meter (Thermo Fisher Scientific, A33978, Inc.).

5-Ethynyl-2'-deoxyuridine (EdU) assay. The EdU assay (Guangzhou RiboBio, C10310-1 Co, Ltd.) was performed

according to the manufacturer's protocols. Briefly, 1x10^4 cells were incubated in 24-well plates for 24 h at 37˚C. A total of 2x103 MDA-MB-231 or MCF-7 cells in 100 μl high-glucose DMEM culture solution per were treated with 50 μM EdU for 2 h at 37˚C. After fixing for 15 min with 4% paraformaldehyde at 37˚C, the cell membranes were permeabilised using 0.5% Triton X-100 for 15 min at 37˚C. A total of 2x103 MDA-MB-231 or MCF-7 cells in 100 μl high-glucose DMEM culture solution per were then treated with 100 μl 100:1 diluted Hoechst 33342 for 30 min at room temperature and imaged using a fluorescence microscope (Nikon Corporation, x40). The images were analysed using ImageJ 1.8.0 (National Institutes of Health).

RNA extraction and reverse transcription-quantitative PCR (RT-qPCR). According to the manufacturer's protocol, TRIzol® (Invitrogen, 15596018) was added to the different cell lines to extract total RNA. All RNA samples were dissolved in DEPC water (Beyotime Institute of Biotechnology). The quality and concentration of total RNA was detected using NanoDrop® ND-1000 (Thermo Fisher Scientific, Inc.). The total RNA was then reverse transcribed using the PrimeScript™ RT reagent kit (37˚C 15 min; 85˚C 5 sec; 4˚C for 5 min, Takara Bio, Inc.). SYBR Green qPCR Master Mix (Takara Bio, Code No. RR430S RR430A, Inc.) was added to the generated cDNAs alongside the specific primers (obtained from TsingKe Biotechnology, Co., Ltd.), which were all dissolved in DEPC to a final volume of 10 μl (95˚C 30 sec; 95˚C 5 sec; 60˚C 30 sec, number of cycles: 40; 95˚C 15 sec, 60˚C 60 sec, 95˚C 15 sec). This system was then added to a 96-well plate and tested using a LightCycler 480® Real Time PCR System (Roche Diagnostics). Each reaction was tested ≥ three times. Non-specific amplification was detected using a dissolution curve. The sequences of the primers used were: TRPC5OS forward, 5'-TCATTGATGGACTTGTTGCTTG-3' and reserve, 5'-AAGTCTGAGAGATCAGGGAGAT-3' and GAPDH (glyceraldehyde-3-phosphate dehydrogenase) forward, 5'-GCTGCGAAGTGGAAACCTAC-3' and reverse, 5'-CCTCCTTCTGCACACATTTGAA-3'. The quantification method used for mRNA expression was comparative Cq method (19).

High-throughput sequencing. The RNA was extracted as aforementioned following TRPC5OS overexpression. Agarose gel electrophoresis was used for assessing the integrity of the extracted RNAs, whereas quantification and further quality tests were performed using a NanoDrop® ND-1000 (Thermo Fisher Scientific, Inc.). Subsequently, an NEB Next® Poly (A) mRNA Magnetic Isolation Module (New England BioLabs, E7490L, Inc.) was used for mRNA enrichment by adding to the total RNA extract. A library of the processed RNA product was established using the KAPA Stranded RNA-Seq Library Prep kit (KK8401, Roche Diagnostics). The loading concentration of the final library was ≥200 ng/μl and total RNA was ≥2.5 μg. The sequence was generally greater than 200 nt, the direction of sequencing is 5'-3'. The established library was sequenced using SeqPlex RNA amplification Kit (SEQR-50RXN, Merck, Inc) on the Illumina HiSeq 4000 platform (Illumina, Inc.). The data was analysed by SUPPA2.0, Cytoscape 3.6.1 and cd-hit-v4.8.1.

Bioinformatics analysis of differentially expressed genes (DEGs), screening the top 10 Gene Ontology (GO) and Kyoto Encyclopaedia of Genes and Genomes (KEGG). To explore the possible mechanism by which TRPC5OS exerts its effects, bioinformatics analysis was performed. Principal component analysis (PCA) was performed with princomp function of R (http://www.r- project.org/) in this experience. Scale function was used to perform z-score processing on expression spectrum before PCA dimensionality reduction. PC1 and PC2 are principal components 1 and 2 respectively, which are the two principal components with the highest proportion after dimensionality reduction and clustering by PCA algorithm. The GO database was used to perform GO functional enrichment analysis for the DEGs (www.geneontology.org). GO terms were sorted by their enrichment scores [-$\log_{10}$ (P-value)] before the top 10 terms were selected for further analysis ('P-value' stands for the fisher exact test value of the term and was calculated by DAVID databases after DEGs were inputted into). KEGG analysis was used to identify the pathways in which the DEGs were enriched (https://www.kegg.jp/), where the top 10 KEGG terms were sorted and selected for further analysis. We input DEGs that exhibited >1.5-fold change in expression into DAVID databases for GO and KEGG analysis.

In addition, protein-protein interactions (PPIs) were analysed to elucidate the interactions among the targeted genes using Search Tool for the Retrieval of Interacting Genes/Proteins (STRING; www.string-db.org/; active interaction sources: Textmining, Experiments, Databases, Co-expression, Neighborhood, Gene Fusion, Co-occurrence; required interaction score: 0.40). The network nodes represented proteins, whereas the edges between nodes represented PPIs. PPI enrichment P-value <0.05 means that proteins were defined as interactions among themselves. GEPIA 2 (www.gepia2.cancer-pku.cn/) was used to analyse the expression of enolase 1 (ENO1) in tumour and normal tissue samples(from the Jiangsu Province Hospital). Kaplan-Meier curves followed by a log-rank test of the overall survival of patients with breast cancer were analysed using KMplot (kmplot.com/analysis/). The patient survival data of KMplot came from GEO, EGA, and TCGA.

Western blotting. After cells were transfected with the TRPC5OS lentivirus, protein extraction was performed using RIPA Lysis Buffer (Beyotime Institute of Biotechnology). Total protein concentration in the supernatant was determined with Bicinchoninic Acid assay (Beyotime biotechnology, China). SDS-PAGE Sample Loading Buffer (Beyotime Institute of Biotechnology) was added to the protein lysates and boiled to 95˚C for 5 min. These protein samples (10 ul/well) were resolved using 10% SDS-PAGE and transferred onto PVDF. Subsequently, the membranes were blocked in QuickBlock™ Blocking Buffer for Western Blotting (Beyotime Institute of Biotechnology) for 15 min at room temperature. These membranes were then incubated with an anti-β-actin (Abcam, ab179467, 1:5,000) or anti-TRPC5OS antibody (Dia-an Biological Technology Incorporation; NP_001182505, 1:5,000) at 4˚C for 12-14 h. Subsequently, the membranes were washed three times and then incubated with HRP-conjugated Affinipure Goat Anti-Mouse and Anti-Rabbit IgG antibodies (H+L; SA00001-2; SA00001-1; ProteinTech Group, Inc) for

2 h. The bands were observed by ECL chemiluminescence substrate (Biosharp, BL520A). Densitometry analysis was performed using ImageJ 1.8.0.

Co-immunoprecipitation assay (Co-IP). Co-IP was performed using anti-TRPC5OS (Dia-an Biological Technology Incorporation; catalog number: NP_001182505) or rabbit IgG (control) (Thermo Fisher Scientific, Inc. catalog number: 88804) antibodies using a classic magnetic Co-IP kit according to the manufacturer's protocol (Thermo Fisher Scientific, Inc. catalog number: 88804). First, 10 μg antibody was incubated with the 1,000 ug protein in the cell lysate in a final volume of 500 μl. This mixture was incubated on a wheel at 4˚C overnight. A total of 250 μg magnetic beads (IP antibody binds to protein A/G magnetic microbeads) conjugated to anti-TRPC5OS or rabbit IgG (control) antibodies were added into a 1.5-ml centrifuge tube, Wash Buffer was used to clean the magnetic beads three times. Subsequently, the protein-antibody mixture was added this a centrifuge tube and mixed with the magnetic beads. This mixture was then incubated at room temperature for 1 h on rotation. Place the tubes on a magnetic separator (i.e. Millipore Cat. # 20-400) and discard the supernatant after bead aggregation. Remove the tubes from the magnet. Add 0.5 ml of Wash Buffer to each tube and vortex briefly for three times. In total, 100 μl Low pH Elution Buffer was then added to the centrifuge tube and incubated for 10 min at room temperature. The supernatant was collected by centrifugation at 4˚C, 14,000 x g for 1 min, and magnetic beads were thrown away. The proteins eluted using the anti-TRPC5OS or rabbit IgG (control) antibodies were then analysed using the Fast Silver Stain Kit (Fig. S1; Beyotime Institute of Biotechnology; catalog number: P0017S). These protein samples were then loaded into 10% SDS-PAGE gels with 30 ul per well, and staining gels at 4˚C for 3 min. Liquid chromatography (LC)-mass spectrometry (MS)/MS was performed using these last eluted supernatant immunoprecipitated proteins.

LC-MS/MS. The protein was extracted using RIPA Lysis Buffer and the protein concentration of the samples were determined by using BCA Protein Assay Kit (Beyotime Institute of Biotechnology). Next, the samples underwent enzyme hydrolysis in solution and gel using formic acid (Fisher Scientific; A117-50); acetonitrile (Fisher Scientific; A955-4); trypsin (Promega; V528A); sep-Pak C18 Desalination column (Waters; WAT200685); Peptides capture column Acclaim PepMap C18, 100 μm x20 mm (Thermo Scientific; cat. no. 164946); Peptides analytical column Acclaim PepMap C18, 75 μm x250 mm (Thermo Scientific; 164569). Appropriate volume 10 mmol/l DTT was added and placed in 56˚C water bath for 60 min. After cooling to room temperature, all liquid was absorbed, and then appropriate volume 55 mmol/l IAA was added and placed away from light for the 45 min at room temperature. Pancreatic enzyme solution was added and placed at 4˚C for 30 min. Whereafter, 25 mmol/l NH4HCO3 was added and placed in 37˚C water bath overnight. After enzymatic hydrolysis, solid phase extraction enrichment and purification were performed. In LC-MS/MS (Q-Exactive liquid chromatograph- mass spectrometer (Thermo Fisher Scientific, Inc.); Ion transport tube temperature was 320˚C), the samples were separated on a Poroshell 120 C18 column (2.7 μm; 2.1x30 mm; Agilent Technologies, Inc, 689975-302). The mobile phase consisted of the A phase (0.1% formic acid/pure water) and the B phase (100% acetonitrile). The flow rate of the mobile phase was 0.3 ml/min and the concentration gradient was 10% (0 min), 10% (1 min), 90% (4 min), 90% (8 min) and 10% (9 min) of the B phase. A total of 5 μl were injected each time. The mass spectrometer was connected to an ion source and the positive ionisation mode of the multiple reaction monitoring mode (MRM) was selected. Both Q1 and Q3 were set at Unit resolution. The flow rate of the drying gas (nitrogen) was 10 l/min and its temperature was maintained at 350˚C. The optimum capillary voltage was 5,500 V. The atomiser pressure was set to 35 psi. Data were collected and processed using an AB SCIEX Workstation Software (pAnalyst 1.62, Shanghai AB SCIEX Analytical Instrument Trading Co.). The peptides were monitored in the MRM.

Statistical analysis. Data from clinical tissue samples of 30 patients were compared using a paired t-test. One-way ANOVA was used for comparing among multiple groups and the Tukey's post hoc test was used. Numerical data are presented as the mean ± standard deviation. $P<0.05$ was considered to indicate a statistically significant difference. Statistical analysis was performed using SPSS version 20 (IBM Corp.). Each experiment was independently repeated three times except for RNA sequencing.

Results

TRPC5OS expression in the TNBC tissue samples and breast cancer cell lines. To measure the expression of TRPC5OS in tissue samples of patients with TNBC and in a panel of different breast cancer cell lines, mRNA expression levels of TRPC5OS were detected using RT-qPCR. As shown in Fig. 1A, the mRNA expression levels of TRPC5OS in TNBC tumour tissues were significantly higher compared with those in the adjacent normal tissues. In addition, TRPC5OS expression was found to be significantly higher in tissue samples from larger masses of tumours (≥3 cm; Fig. 1B). However, there was no difference in TRPC5OS expression between tissues from different histological grades (II and III; Fig. 1C). Among the different breast cancer cell lines, the mRNA expression levels of TRPC5OS were generally higher compared with those in the normal breast cell line MCF-10A. However, compared with other breast cancer cells such as ZR-75-1, MDA-MB-453, SK-BR-3, JIMT-1, BT474, the mRNA expression levels of TRPC5OS were significantly higher in TNBC cell lines, such as SUM-1315 and MDA-MB-231 (Fig. 1D).

Transfection efficiency of lentiviral constructs in MDA-MB-231 and MCF-7 cells. To verify the transfection efficiency of the lentiviral constructs, fluorescence microscopy, western blotting and RT-qPCR were performed following transfection and treatment with puromycin for 2 weeks. Green fluorescence protein expression was observed in >90% transfected cells (Fig. 2A). The green fluorescence comes from a fluorescent gene carried by the lentivirus itself. RT-qPCR analysis demonstrated that both in MDA-MB-231 and MCF-7 cells, the mRNA expression levels of TRPC5OS were significantly higher in TRPC5OS-overexpressing cells compared with the

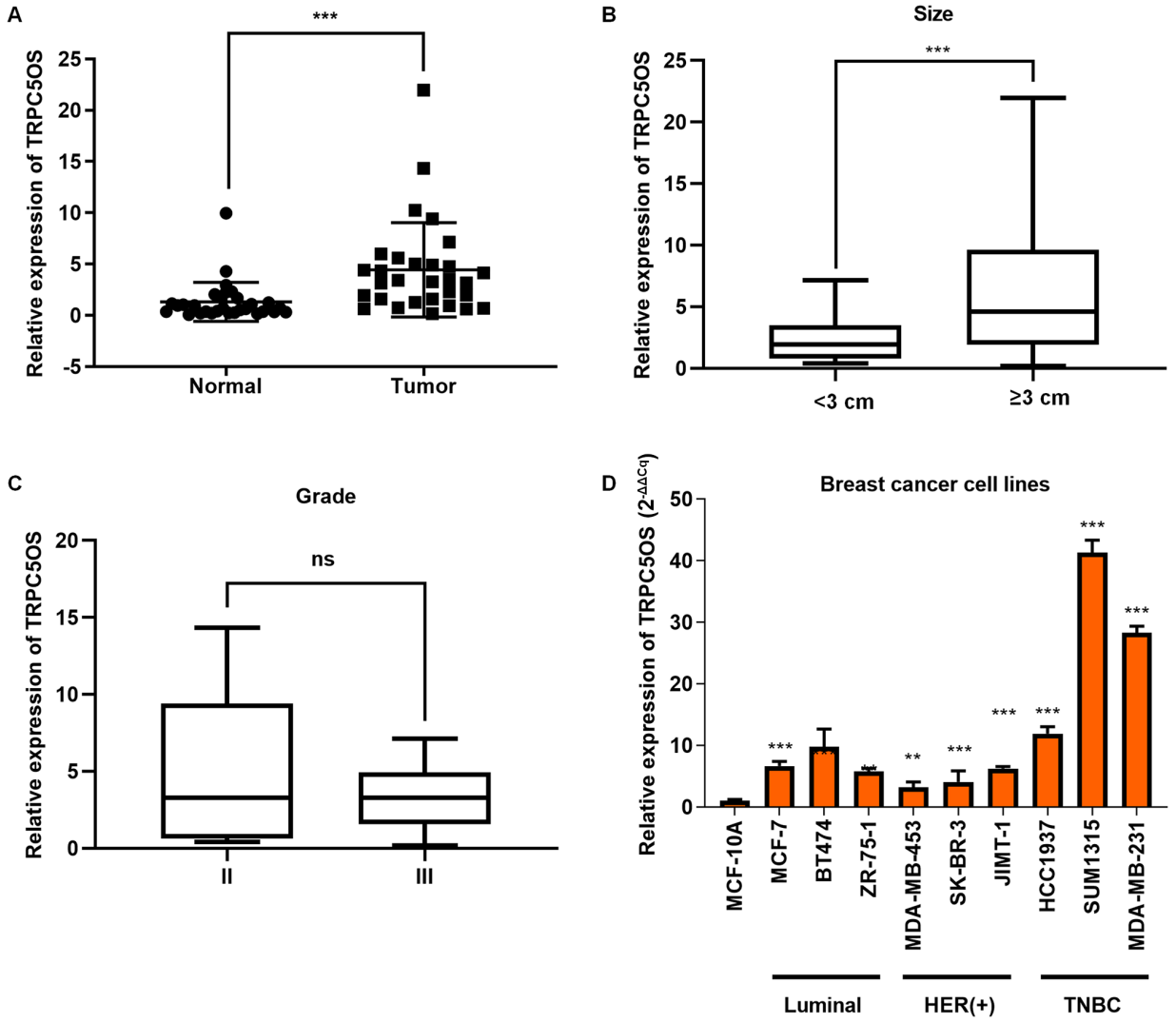

Figure 1. TRPC5OS expression in the tissue samples of patients with TNBC and in a panel of breast cancer cell lines. (A) mRNA expression levels of TRPC5OS were detected in the tissues of patients with TNBC using reverse transcription-quantitative PCR. (B) The relationship between tumour size and TRPC5OS expression levels was calculated, where a tumour size cut-off value of 3 cm was used. (C) Relationship between histological grade and TRPC5OS expression levels following stratification. (D) mRNA expression levels of TRPC5OS in MCF-10A normal mammary epithelial cells compared with nine different breast cancer cell lines. HER-2(-), ER(+) cell lines were MCF-7, BT-474, ZR-75-1, where the HER-2(+) cell lines were MDA-MB-453, SK-BR-3, JIMT-1. TNBC cell lines were HCC1937, SUM1315 and MDA-MB-231. Each experiment was repeated ≥ three times. **P<0.01 and ***P<0.001 vs. MCF-10A. TNBC, triple-negative breast cancer; TRPC5OS, Transient receptor potential channel 5 opposite strand.

control cells (transfection of empty virus), whereas its expression was significantly decreased in cells with TRPC5OS expression knocked down (Fig. 2B). Western blotting subsequently showed that in MDA-MB-231 and MCF-7 cells, the protein expression level of TRPC5OS was significantly increased by LV-TRPC5OS transfection compared with that in its corresponding LV5 control (Fig. 2C and D). By contrast, it was significantly decreased by LV-193 transfection compared with that in its corresponding LV3 control (Fig. 2C and D). These results suggest that lentiviral transfection was effective in MDA-MB-231 and MCF-7 cells.

TRPC5OS promotes proliferation of breast cancer cells. CCK-8 and EdU assays were next performed to detect the biological function of TRPC5OS in MDA-MB-231 and MCF-7 cells. CCK-8 assay results revealed that the proliferative ability was markedly increased following TRPC5OS overexpression but it was decreased following TRPC5OS knockdown (Fig. 3A and B) in MDA-MB-231 cells compared with those in their corresponding negative controls. The results of the CCK-8 assay in MCF-7 cells were consistent with those of MDA-MB-231 cells (Fig. 3C and D). EdU results also showed that cell viability was significantly increased in TRPC5OS-overexpressing cells, whereas it was significantly decreased following TRPC5OS knockdown (Fig. 3C), compared with those in their corresponding negative controls. Therefore, these results suggest that the viability and proliferative abilities of MDA-MB-231 cells were promoted by TRPC5OS overexpression.

Identification of DEGs following TRPC5OS overexpression. To further investigate the effects of TRPC5OS overexpression, high-throughput sequencing was used to screen for the DEGs following TRPC5OS overexpression in MDA-MB-231 cells.

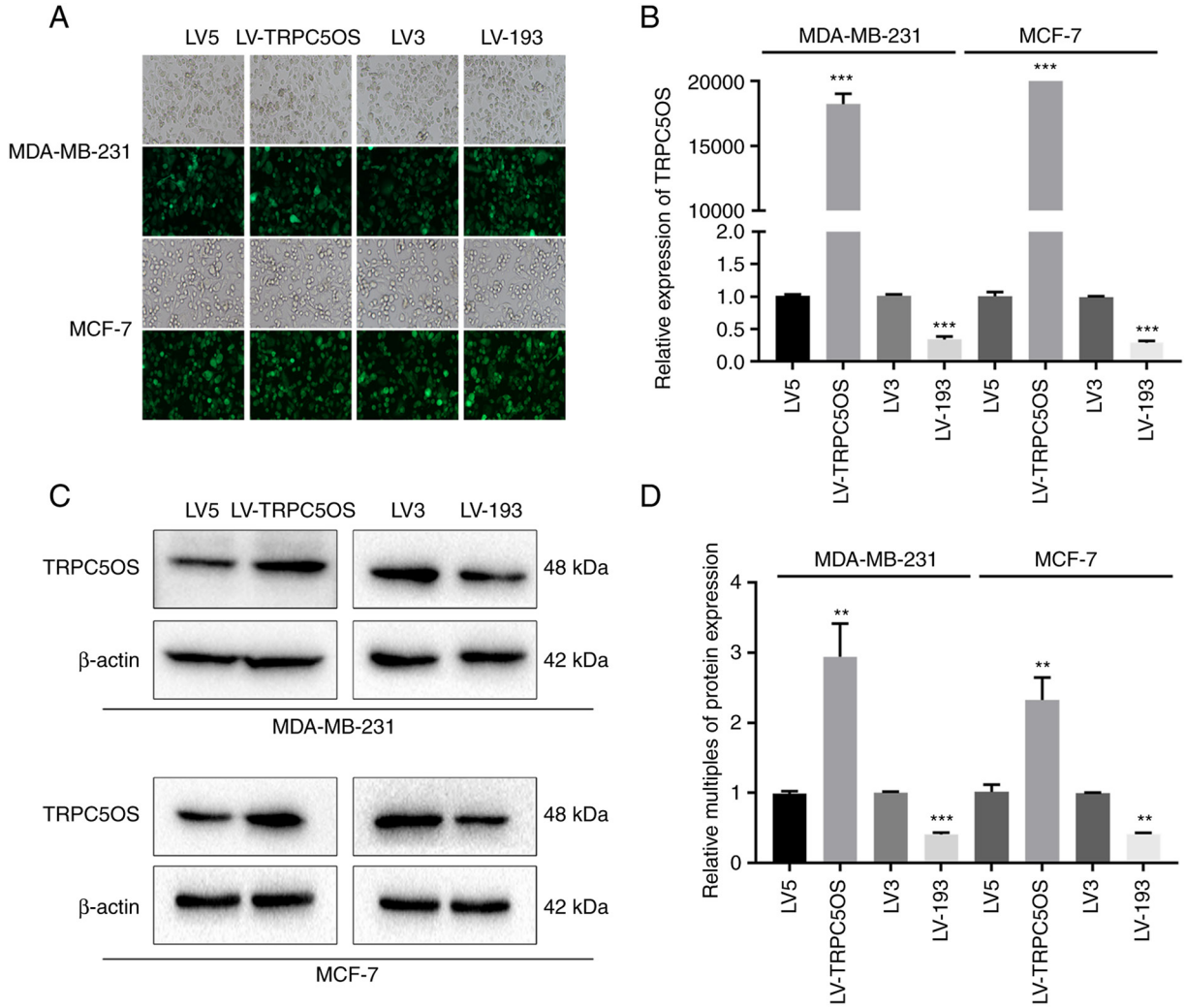

Figure 2. Verification of lentivirus transfection efficiency. (A) GFP expression was observed in >90% of cells using fluorescence microscopy. (B) Reverse transcription-quantitative qPCR was performed to measure the mRNA expression levels of TRPC5OS. (C) The protein expression levels of TRPC5OS were detected using western blotting. (D) Densitometry analysis of TRPC5OS protein expression was calculated using ImageJ and the differences in expression are expressed as the fold change. Each experiment was repeated ≥ three times. **P<0.01 and ***P<0.001 (LV5 vs LV-TRPC5OS; LV3 vs LV-193). TRPC5OS, Transient receptor potential channel 5 opposite strand; LV, lentivirus.

The top 10 of upregulated and downregulated DEGs are shown in the supplemental material (Table SII). Inter-group comparison and cluster analysis were then performed according to the fragments per kilobase of exon per million values of significant DEGs, where heat map was generated showing the gene expression pattern in the two different samples. There were significant differences between control (LV5) and TRPC5OS overexpressed MDA-MB-231 cell line (Fig. 4A). A scatter plot also described the overall distribution trend in the two samples. The results showed that a total of 5,256 genes were differentially expressed, including 3,269 upregulated genes and 1,987 downregulated genes (fold change ≥1.5; Fig. 4B). The principal component analysis results showed the difference between control (LV5) and TRPC5OS overexpressed (LV-TRPC5OS) MDA-MB-231 cell line. Significant differences in the expression data were shown in Fig. 4C between control (LV5) and TRPC5OS overexpressed (LV-TRPC5OS) MDA-MB-231 cell line. Correlation between the two samples can be seen in the heatmap diagrams of the sample correlation coefficients and indicated that the similarity of the two samples was high, the experiment was reliable, and the sample selection was reasonable (r-value >0.92; Fig. 4D).

GO and KEGG analysis of DEGs. To further investigate whether these differential genes could serve a role in cancer proliferation, GO and KEGG analyses were performed to identify the biological functions and pathways associated with these aberrantly expressed genes. GO analysis revealed that the biological processes most commonly associated with the upregulated genes generally took part in the 'cell division' and 'DNA replication' processes (Figs. 5A and S1A). By contrast, the biological processes most commonly associated with the downregulated genes were involved in 'neutrophil degranulation' and 'cell proliferation regulation' (Figs. 5B and S1C). The upregulated genes were primarily associated with the 'cytosol', 'nucleoplasm' and 'centrosome' compartments (Fig. 5A), whereas the downregulated genes were primarily associated with the 'extracellular exosome' and 'endoplasmic reticulum lumen' compartments (Fig. 5B). The molecular functions of the upregulated genes were primarily associated with 'protein

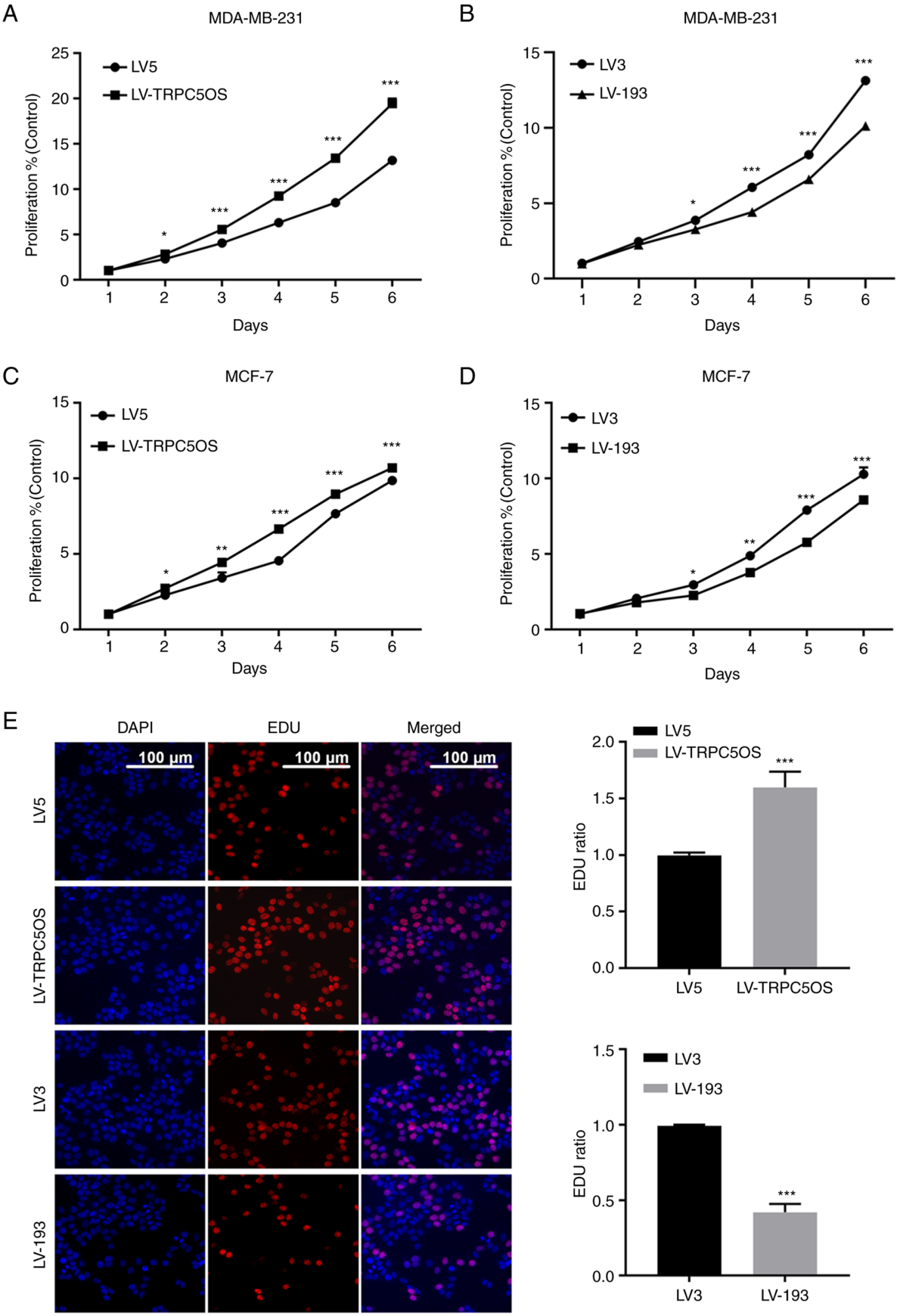

Figure 3. TRPC5OS overexpression increases the proliferative ability of breast cancer cells. The proliferative ability of MDA-MB-231 cells was assessed using a Cell Counting Kit-8 assay following (A) LV5, LV-TRPC5OS, (B) LV3 or LV-193 transfection. The proliferative ability of MCF-7 cells was assessed using a Cell Counting Kit-8 assay following (C) LV5, LV-TRPC5OS, (D) LV3 or LV-193 transfection. (E) An EdU-incorporation assay was used to detect the proliferative ability of MDA-MB-231 cells following LV5, LV5-TRPC5OS, LV3 or LV-193 transfection. Scale bar, 100 μm. Each experiment was repeated at least three times. *P<0.05, **P<0.01 and ***P<0.001 (LV5 vs LV-TRPC5OS; LV3 vs LV-193). TRPC5OS, Transient receptor potential channel 5 opposite strand; LV, lentivirus.

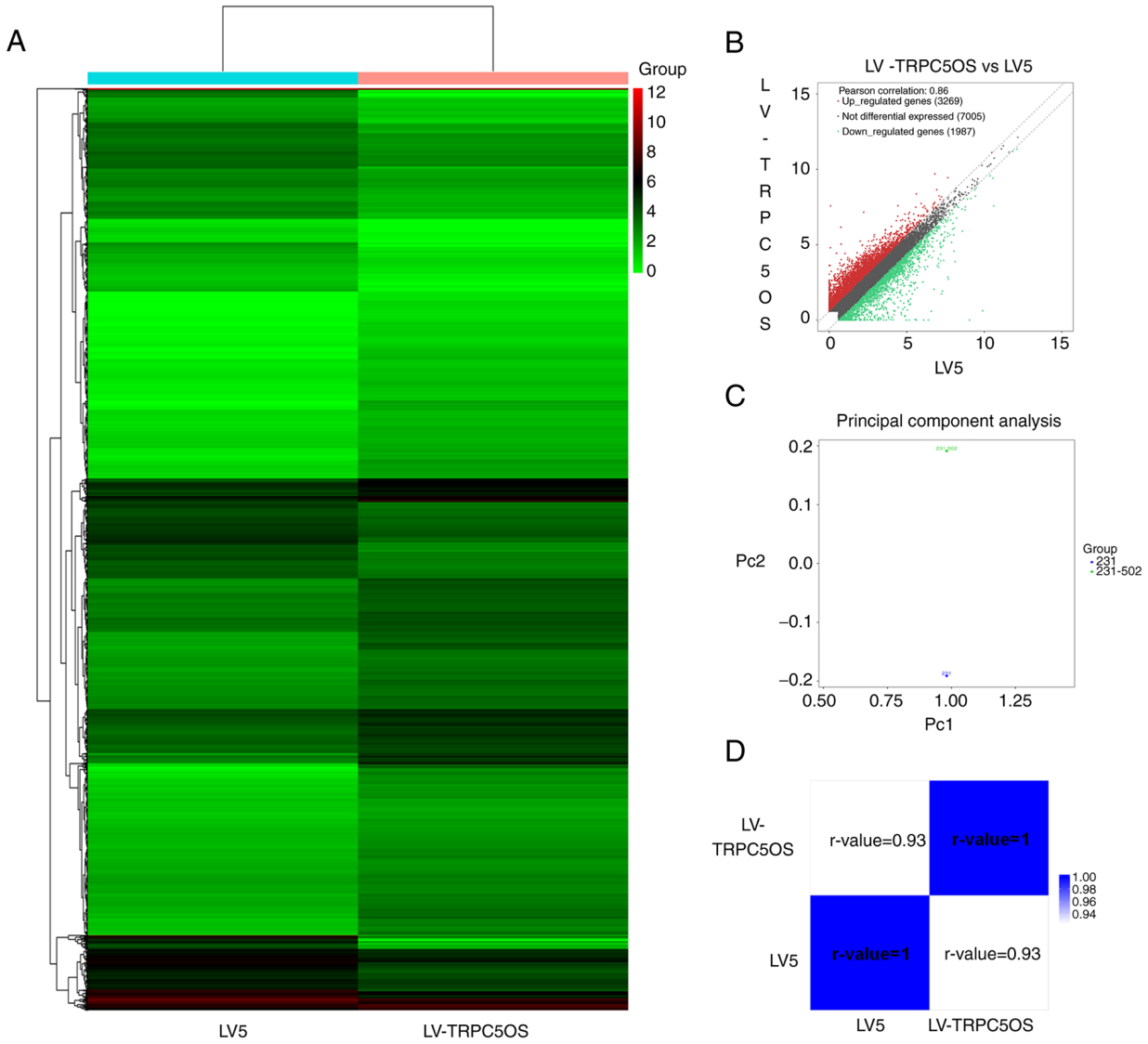

Figure 4. Differentially expressed genes between the LV5 and TRPC5OS-overexpressing groups of MDA-MB-231 cells. (A) Differentially expressed genes between LV5-transfected and TRPC5OS-overexpressing cells are shown in the heat map. Each row represents a gene, whereas each column represents a sample. Red represents significantly upregulated genes, whereas green represents significantly downregulated genes. (B) The overall distribution trend of the two samples can be seen in the scatter chart. Each dot in the scatter plot represents a gene, where the X- and Y-axis coordinates represent the fragments per kilobase of exon per million mapped fragments expression values of the genes in the two samples. The two diagonal lines delineate the upregulation (upward site), downregulation(downward site), and unaltered (middle) genes. (C) Principal component analysis results showed the classification of expression profiles between the samples. Genes with a significant difference (One-way ANOVA and Tukey's post hoc test) in all samples were used for principal component analysis. Each colour represents one group, and each axis represents a principal component. (D) Correlation analysis was calculated to determine the similarity between LV5 and LV-TRPC5OS transfected samples. The depth of blue represents the degree of correlation. The closer the Pearson correlation coefficient is to 1, the higher the similarity between the two samples. TRPC5OS, Transient receptor potential channel 5 opposite strand; LV, lentivirus.

binding', 'RNA binding' and 'ATP binding' (Fig. 5A), whilst those associated with the downregulated genes included 'protein binding' and '2'-5'-oligoadenylate synthetase activity' (Fig. 5B). The pathways of these aberrantly expression genes were then explored using KEGG analysis. The pathways of the upregulated genes included 'homologous recombination', the 'Fanconi anaemia pathway', 'one carbon pool by folate', 'inositol phosphate metabolism', 'pancreatic cancer' and 'pyruvate metabolism' (Figs. 5C and S1B). The biological pathways of the downregulated genes included 'lysosome', the 'TNF signalling pathway', the 'HIF-1 signalling pathway', 'transcriptional misregulation in cancer' and 'hepatitis B' (Figs. 5C and S1D).

Prediction of target proteins following TRPC5OS overexpression. To identify the potential target proteins following TRPC5OS overexpression, Co-IP was performed. There was an obvious band near 40 kDA in TRPC5OS overexpression group which indicated that the molecular weight of the protein interacted with TRPC5OS was close to 40 kDA (Fig. S2) before the targeted proteins were predicted based on LC-MS/MS analysis. Differential proteins that were identified at least twice out of the three runs were selected. The results revealed that 17 potential interacting targets of TRPC5OS were identified, including Annexin A1 (ANXA1), peroxiredoxin 1 (PRDX1), enolase 1 (ENO1), LDHB (lactate dehydrogenase B), YWHAQ (tyrosine 3-monooxygenase/tryptophan

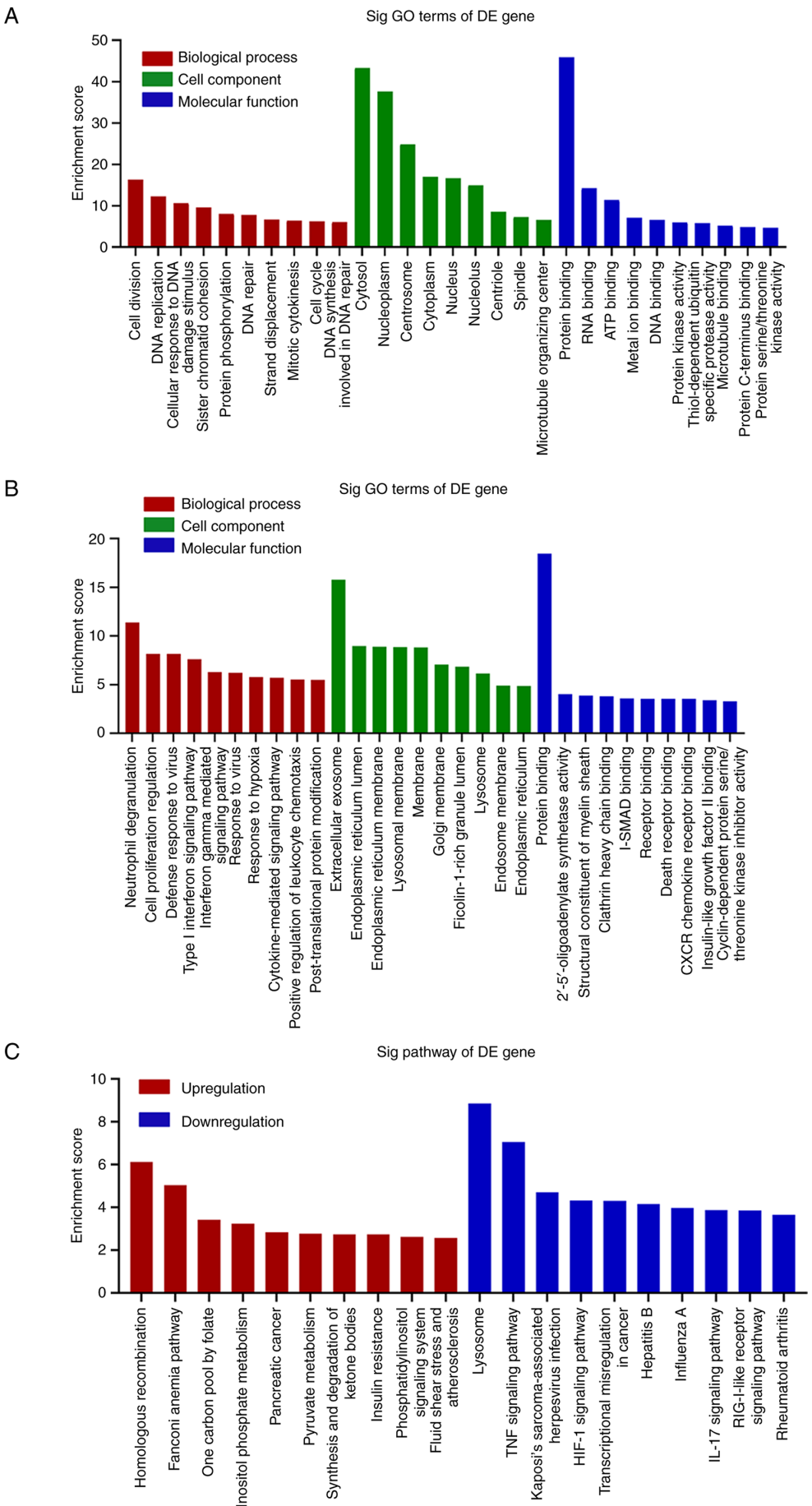

Figure 5. GO and KEGG pathway analysis of DEGs. GO analysis of the (A) upregulated and (B) downregulated DEGs are listed. (C) KEGG analysis of upregulated and downregulated DEGs is presented. GO, Gene Ontology; KEGG, Kyoto Encyclopaedia of Genes and Genomes; DE, differentially expressed; DEG, differentially expressed genes; sig, significant.

5-monooxygenase activation protein theta), FLNC (filamin C), VDAC1 (voltage dependent anion channel 1), eukaryotic translation elongation factor 1 γ (EEF1G), ribosomal protein L7a), RPS3 (ribosomal protein S3), PCBP2 [poly(rC) binding protein 2], CCT6A (chaperonin containing TCP1 subunit 6A), CS (citrate synthase), HNRNPD (heterogeneous nuclear ribonucleoprotein D), AKR7A2 (aldo-keto reductase family 7 member A2), CALR (calreticulin) and LCN1 (lipocalin 1) (Table SIII). Subsequently, PPI network analysis was performed to analyse the interactome of these 17 differentially-expressed proteins. Proteins with the most interactions were selected, including ENO1, PRDX1 and EEF1G (Fig. 6A).

Interactions between the DEGs and proteins. Subsequently, three biological processes associated with proliferation from GO analysis were selected, namely cell division, RNA replication and negative regulation of cell proliferation. The genes enriched in these biological processes were then subjected to PPI analysis with the target proteins. The genes that interacted with the target proteins are shown in Fig. 6B. The results showed that the interaction relationship among tumour protein p53, histone deacetylase 1 (HDAC1) and superoxide dismutase 2 (SOD2), all of which are associated with proliferation, were the most significant. Deletion of TP53 has been found to promote glycolysis and tumour cell proliferation (20). A previous study showed that HDAC1 can mediate the acetylation of ENO1, the upregulation of which could promote the biological activity of ENO1 (21) to in turn increase the proliferation of MDA-MB-231 and MCF-7 cells. SOD2 is a mitochondrial enzyme that decreases the levels of reactive oxygen species (ROS) in the mitochondria (22). Low levels of ROS exerts a negative regulatory role on proliferation (23). To conclude, these DEGs aforementioned were all associated with cancer proliferation.

ENO1 may be a potential target protein mediated by TRPC5OS. Due to it exhibiting the most interactions with other target genes and proteins, ENO1 was chosen fo examination as a potential target protein of TRPC5OS. Western blotting revealed that the protein expression of ENO1 was significantly increased following TRPC5OS overexpression, but was significantly decreased following TRPC5OS knockdown compared with that in their corresponding negative controls (Fig. 7A and B). Expression of ENO1 was markedly higher in tumour tissues compared with that in the normal tissues based on GEPIA 2 analysis (Fig. 7C). Kaplan-Meier curves and log-rank tests of the overall survival of patients with breast cancer revealed that high expression levels of ENO1 were associated with poorer prognoses (Fig. 7D). Therefore, these data suggest that TRPC5OS may regulate the expression of ENO1, which may in turn be associated with less favourable outcomes in patients with breast cancer.

Discussion

At present, anthracyclines and taxanes are the primary treatment methods for breast cancer patients (24). However, the prognosis of patients with TNBC remains poor (25). Therefore, it remains necessary to identify novel targets for the treatment of TNBC. In a previous study, it was found that the levels of

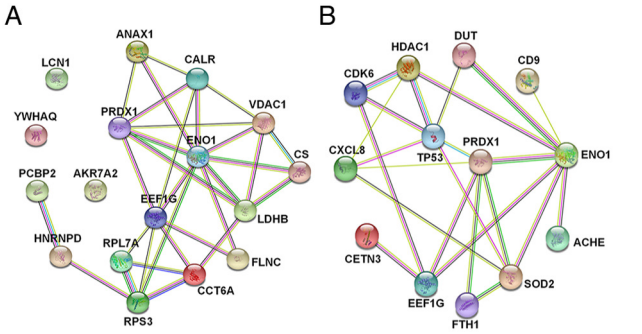

Figure 6. PPI network analysis. (A) PPI network of the targeted proteins was established (ANXA1, PRDX1, ENO1, LDHB, YWHAQ, FLNC, VDAC1, EEF1G, RPL7A, RPS3, PCBP2, CCT6A, CS, HNRNPD, AKR7A2, CALR and LCN1). (B) Genes in the biological processes of Gene Ontology analysis that interacted closely with the targeted proteins were subjected to PPI analysis. PPI, protein-protein interaction; ANXA1, Annexin A1; peroxiredoxin 1 (PRDX1), enolase 1 (ENO1), LDHB (lactate dehydrogenase B), YWHAQ (tyrosine 3-monooxygenase/tryptophan 5-monooxygenase activation protein theta), FLNC, filamin C; VDAC1 (voltage dependent anion channel 1), EEF1G, eukaryotic translation elongation factor 1 γ; RP, ribosomal protein; PCBP2 [poly(rC) binding protein 2], CCT6A (chaperonin containing TCP1 subunit 6A), CS (citrate synthase), HNRNPD (heterogeneous nuclear ribonucleoprotein D), AKR7A2 (aldo-keto reductase family 7 member A2), CALR (calreticulin) and LCN1 (lipocalin 1).

TRPC5OS expression were the highest in MDA-MB-231 cells, where overexpression of TRPC5OS could promote proliferation and viability. Therefore, the present study investigated the potential function mechanism of TRPC5OS by overexpressing it or knocking down its expression in breast cancer cells.

The proliferative ability of MDA-MB-231 and MCF-7 cells was first measured after overexpressing TRPC5OS. The results revealed that TRPC5OS overexpression promoted the proliferation of the breast cancer cells and TRPC5OS knockdown inhibited the proliferation of breast cancer cells. Next, high-throughput sequencing of samples from TRPC5OS-overexpressing MDA-MB-231 cells and cells from the LV5 control group was performed. MDA-MB-231 cells are TNBC cells (26). Current treatment methods for breast cancer include surgery, chemotherapy, radiotherapy, endocrine therapy and targeted therapy (27,28). However, due to the lack of ER, PR and HER-2 expression (29), TNBC is characterized by a unique molecular profile, metastatic pattern, aggressive behavior and lack of an effective targeted therapy, lead to poor prognosis (3-5). Targeting TRPC5OS for therapy may markedly improve the outcome of patients with TNBC. Therefore, MDA-MB-231 cells was used for RNA sequencing. Sequencing with only one cell line has been reported in other studies (30,31). In addition, it was found that TRPC5OS also served as a cancer-promoting role in MCF-7 cells, which is non-TNBC by using EdU) assay. However, in future studies, the interactions between TRPC5OS and target proteins in MCF-7 cells will need to be assessed.

The present study found that there were 5,256 DEGs between the two groups. Among these, 3,269 genes were upregulated and 1,987 genes were downregulated (fold change threshold >1.5). Subsequently, these DEGs were analysed using GO and KEGG. GO analysis revealed that the main biological processes involving these upregulated genes were 'cell division' and 'DNA replication', whereas the main biological

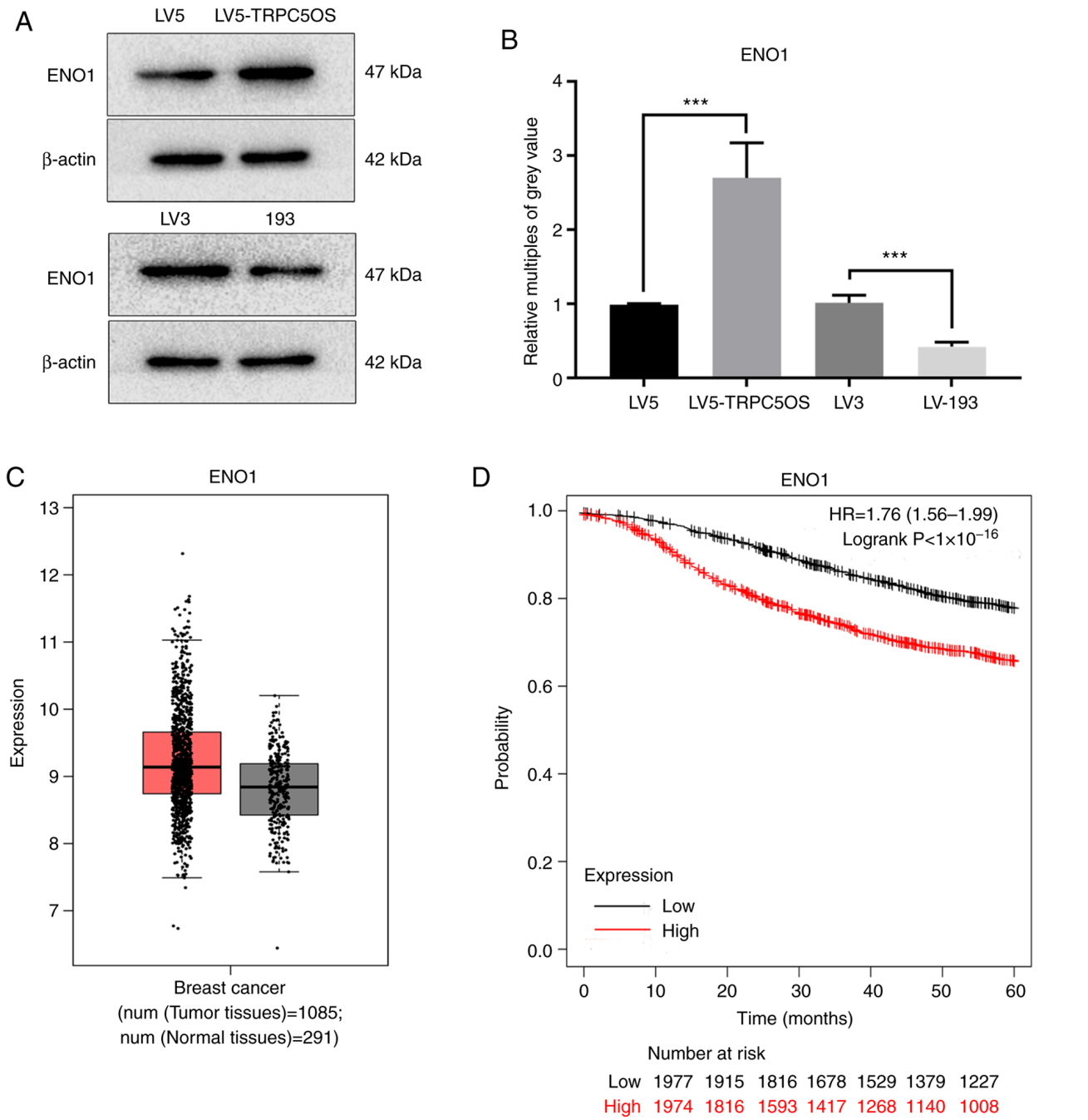

Figure 7. ENO1 expression analysis. (A) The protein expression levels of ENO1 were assessed using western blotting following LV5, LV-TRPC5OS, LV3 or LV-193 transfection. (B) Densitometry analysis of ENO1 protein expression was calculated using ImageJ. (C) Expression levels of ENO1 in tumour and normal tissue samples were analysed using GEPIA 2. (D) Kaplan-Meier curves and log-rank test of the overall survival of patients with breast cancer (median cut-off value). Each experiment was repeated ≥ three times. ***P<0.001. TRPC5OS, Transient receptor potential channel 5 opposite strand; ENO1, enolase 1; LV, lentivirus; HR, hazard ratio.

processes involving the downregulated genes were 'neutrophil degranulation' and 'cell proliferation regulation'. Cell division and DNA replication are closely associated with cell cycle progression and proliferation (32-34), where dysregulation can lead to carcinogensis (35,36). Before DNA replication in the cell cycle, cells need to enter the G_1 phase and release a large number of intracellular signals to regulate cell division (37). During this process, in cases of dysregulation, such as insufficient or excessive chromosomal DNA replication, then cell division and proliferation would not be tightly regulated, resulting in the development of cancer (36).

Subsequent KEGG results showed that the main pathways these upregulated genes were associated with primarily took part in 'homologous recombination', whereas for the downregulated genes, they primarily took part in 'lysosome' and 'TNF signalling pathways'. Gross chromosome rearrangement (GCR) and copy-number variations (CNVs) are the result of incorrect DNA replication and are frequently observed features of cancer (38). Homologous recombination can cause replication restarts, where such recombination-restarted forks have high probabilities of error, leading to DNA replication errors, production of GCRs and gene amplification in cancer (28). In

addition, homologous recombination can result in the production of non-recurrent CNVs in genomic diseases. HR proteins associate with the nascent strand behind the collapsed fork and subsequent strand invasion at the collapse site facilitates accurate HR-dependent fork restart with the correct template (39). There is evidence that the lysosome pathway can regulate cancer proliferation (40). The proliferation of cancer cells leads to energy depletion, which in turn affects their proliferation (41). To overcome this obstacle, cancer cells typically use lysosomes to degrade macromolecules obtained from the microenvironment to produce ATP and synthesise metabolic substrates (42).

In the present study, GO and KEGG analyses revealed that biological processes and pathways are closely associated with proliferation. Therefore, the potential target proteins of TRPC5OS were next explored. Co-IP followed by LC-MS/MS analysis was thereby performed, following which proteins that were detected at least twice were used to establish a PPI network. From the analysis of the PPI network, three target proteins were selected (ENO1, PRDX1 and EEF1G) that had the most interactions and therefore were the most likely to be associated with cancer proliferation. ENO1 functions as a glycolytic enzyme in glycolysis (43,44). Accumulating evidence has reported that ENO1 is closely associated with tumour development (45-47). ENO1 can regulate the proliferation, migration and invasion of glioma cells through the PI3K/Akt pathway (48). PRDX1 is a member of the peroxiredoxin family of antioxidant enzymes (49). The biological function of PRDX1 primarily depends on the proteins that interact with PRDX1, including macrophage migration inhibitory factor (MIF) and peptidylprolyl isomerase A (PPIA) (50). MIF can inhibit the peroxidase activity of PRDX1, whereas PPIA binds to all isoforms of PRDXs to enhance antioxidant activity, leading to tumorigenesis (50). EEF1G is a member of the EEF1 family, which transfers aminoacyl tRNAs to the ribosome (51). Accumulating evidence has shown that EEF1G serves a key role in cancer development (52,53). EEF1G has also been associated with oncogene-induced aging, which is an important mechanism that inhibits tumour formation, to prevent the uncontrolled proliferation of tumour cells under the action of abnormal carcinogenic signals (53). Taken together, it was suggested that ENO1, PRDX1 and EEF1G are all associated with tumorigenesis through the PI3K/AKT pathway, antioxidant activity alterations and OIS, respectively. In addition, interactions between differential genes and proteins were analysed based on the PPIs. Amongst ENO1, PRDX1 and EEF1G, given that ENO1 was closely associated with proliferation and had the most interactions with other target genes and proteins, it was considered to be a potential target protein downstream of TRPC5OS.

In conclusion, the function, biological processes and signalling pathways associated with TRPC5OS in TNBC were investigated in the present study, In addition, potential target proteins and interactions between differential genes and target proteins were analysed, which provided guidance and direction for future studies experiments. However, the lack of analysis in > one sample per cell line for RNA sequencing is a limitation to the present study. Additional samples should be analyzed to rule out any false positive. Results from the present study suggest that TRPC5OS may serve as a novel therapeutic target for the treatment of breast cancer. Therefore, exploring the mechanisms by which TRPC5OS regulates TNBC cell proliferation may provide novel insights for the development of clinically viable therapeutic strategies.

Acknowledgements

Not applicable.

Funding

The present study was financially supported by the National Natural Science Foundation of China (grant nos. 81672612 and 81903653), Project of Invigorating Health Care through Science, Technology and Education (Jiangsu Provincial Medical Youth Talent; grant nos. QNRC2016095 and FRC201758), the Project of Nanjing Medical and Science Development (grant nos. 201803014 and YK17179) and the Beijing Medical Award Foundation (grant no. YXJL-2021-0028-0279).

Availability of data and materials

The data generated in the present study may be found in the Gene Expression Omnibus under accession number GSE181330 or at the following URL: https://www.ncbi.nlm.nih.gov/geo/query/acc.cgi?acc=GSE181330.

Authors' contributions

SW, and ZYF participated in the design of the study. XH provided the idea of the project and participated in the design of the experimental scheme. JHP, YH, SBP, YQX, MJZ, WBZ and YYC performed the experiments. MMW, XWW, HX, LLY, XH and HTF contributed to data collection and analysis. HX and ZYF confirm the authenticity of all the raw data. All authors were involved in the writing of the article. All authors have read and approved the final manuscript.

Ethics approval and consent to participate

The protocols involving patients were approved by the Ethics Committees of the First Hospital Affiliated Hospital with Nanjing Medical University (approval no. 2010-SR-091). The patients recruited in this research provided written informed consent.

Patient consent for publication

Not applicable.

Competing interests

The authors declare that they have no competing interests.

References

1. DeSantis CE, Ma J, Gaudet MM, Newman LA, Miller KD, Sauer AG, Jemal A and Siegel RL: Breast cancer statistics, 2019. CA Cancer J Clin 69: 438-451, 2019.
2. Bauer KR, Brown M, Cress RD, Parise CA and Caggiano V: Descriptive analysis of estrogen receptor (ER)-negative, progesterone receptor (PR)-negative, and HER2-negative invasive breast cancer, the so-called triple-negative phenotype: A population-based study from the California cancer registry. Cancer 109: 1721-1728, 2007.

3. Kaplan HG, Malmgren JA and Atwood M: T1N0 triple negative breast cancer: Risk of recurrence and adjuvant chemotherapy. Breast J 15: 454-460, 2009.
4. Mersin H, Yildirim E, Berberoglu U and Gülben K: The prognostic importance of triple negative breast carcinoma. Breast 17: 341-346, 2008.
5. Tan AR and Swain SM: Therapeutic strategies for triple-negative breast cancer. Cancer J 14: 343-351, 2008.
6. Dent R, Trudeau M, Pritchard KI, Hanna WM, Kahn HK, Sawka CA, Lickley LA, Rawlinson E, Sun P and Narod SA: Triple-negative breast cancer: Clinical features and patterns of recurrence. Clin Cancer Res 13: 4429-4434, 2007.
7. Cheang MC, Voduc D, Bajdik C, Leung S, McKinney S, Chia SK, Perou CM and Nielsen TO: Basal-like breast cancer defined by five biomarkers has superior prognostic value than triple-negative phenotype. Clin Cancer Res 14: 1368-1376, 2008.
8. Foulkes WD, Smith IE and Reis-Filho JS: Triple-negative breast cancer. N Engl J Med 363: 1938-1948, 2010.
9. Venkatachalam K and Montell C: TRP channels. Annu Rev Biochem 76: 387-417, 2007.
10. Ma X, Chen Z, Hua D, He D, Wang L, Zhang P, Wang J, Cai Y, Gao C, Zhang X, *et al*: Essential role for TrpC5-containing extracellular vesicles in breast cancer with chemotherapeutic resistance. Proc Natl Acad Sci USA 111: 6389-6394, 2014.
11. Zhang P, Liu X, Li H, Chen Z, Yao X, Jin J and Ma X: TRPC5-induced autophagy promotes drug resistance in breast carcinoma via CaMKKβ/AMPKα/mTOR pathway. Sci Rep 7: 3158, 2017.
12. Dong Y, Pan Q, Jiang L, Chen Z, Zhang F, Liu Y, Xing H, Shi M, Li J, Li XY, *et al*: Tumor endothelial expression of P-glycoprotein upon microvesicular transfer of TrpC5 derived from adriamycin-resistant breast cancer cells. Biochem Biophys Res Commun 446: 85-90, 2014.
13. Ma X, Cai Y, He D, Zou C, Zhang P, Lo CY, Xu Z, Chan FL, Yu S, Chen Y, *et al*: Transient receptor potential channel TRPC5 is essential for P-glycoprotein induction in drug-resistant cancer cells. Proc Natl Acad Sci USA 109: 16282-16287, 2012.
14. Fagerberg L, Hallström BM, Oksvold P, Kampf C, Djureinovic D, Odeberg J, Habuka M, Tahmasebpoor S, Danielsson A, Edlund K, *et al*: Analysis of the human tissue-specific expression by genome-wide integration of transcriptomics and antibody-based proteomics. Mol Cell Proteomics 13: 397-406, 2014.
15. Wichman L, Somasundaram S, Breindel C, Valerio DM, McCarrey JR, Hodges CA and Khalil AM: Dynamic expression of long noncoding RNAs reveals their potential roles in spermatogenesis and fertility. Biol Reprod 97: 313-323, 2017.
16. Lu CW, Zhou DD, Xie T, Hao JL, Pant OP, Lu CB and Liu XF: HOXA11 antisense long noncoding RNA (HOXA11-AS): A promising lncRNA in human cancers. Cancer Med 7: 3792-3799, 2018.
17. Jiang M, Qiu N, Xia H, Liang H, Li H and Ao X: Long noncoding RNA FOXD2AS1/miR1505p/PFN2 axis regulates breast cancer malignancy and tumorigenesis. Int J Oncol 54: 1043-1052, 2019.
18. Breast Cancer Association Consortium; Mavaddat N, Dorling L, Carvalho S, Allen J, González-Neira N, Keeman R, Bolla MK, Dennis J, Wang Q, *et al*: Pathology of tumors associated with pathogenic germline variants in 9 breast cancer susceptibility genes. JAMA Oncol 8: e216744, 2022.
19. Schmittgen TD and Livak KJ: Analyzing real-time PCR data by the comparative C(T) method. Nat Protoc 3: 1101-1108, 2008.
20. Hitosugi T, Zhou L, Elf S, Fan J, Kang HB, Seo JH, Shan C, Dai Q, Zhang L, Xie J, *et al*: Phosphoglycerate mutase 1 coordinates glycolysis and biosynthesis to promote tumor growth. Cancer Cell 22: 585-600, 2012.
21. Arito M, Nagai K, Ooka S, Sato T, Takakuwa Y, Kurokawa MS, Sase T, Okamoto K, Suematsu N, Kato T, *et al*: Altered acetylation of proteins in patients with rheumatoid arthritis revealed by acetyl-proteomics. Clin Exp Rheumatol 33: 877-886, 2015.
22. Yuan L, Mishra R, Patel H, Abdulsalam S, Greis KD, Kadekaro AL, Merino EJ and Garrett JT: Utilization of reactive oxygen species targeted therapy to prolong the efficacy of BRAF inhibitors in melanoma. J Cancer 9: 4665-4676, 2018.
23. Prasad S, Gupta SC and Tyagi AK: Reactive oxygen species (ROS) and cancer: Role of antioxidative nutraceuticals. Cancer Lett 387: 95-105, 2017.
24. McDonald ES, Clark AS, Tchou J, Zhang P and Freedman GM: Clinical diagnosis and management of breast cancer. J Nucl Med 57 (Suppl 1): 9S-16S, 2016.
25. Yin L, Duan JJ, Bian XW and Yu SC: Triple-negative breast cancer molecular subtyping and treatment progress. Breast Cancer Res 22: 61, 2020.
26. Abdelmalek CM, Hu Z, Kronenberger T, Küblbeck J, Kinnen FJM, Hesse SS, Malik A, Kudolo M, Niess R, Gehringer M, *et al*: Gefitinib-tamoxifen hybrid ligands as potent agents against triple-negative breast cancer. J Med Chem 65: 4616-4632, 2022.
27. Paskins Z, Bromley K, Lewis M, Hughes G, Hughes E, Hennings S, Cherrington A, Hall A, Holden MA, Stevenson K, *et al*: Clinical effectiveness of one ultrasound guided intra-articular corticosteroid and local anaesthetic injection in addition to advice and education for hip osteoarthritis (HIT trial): Single blind, parallel group, three arm, randomised controlled trial. BMJ 377: e068446, 2022.
28. Chen P, Ning X, Li W, Pan Y, Wang L, Li H, Fan X, Zhang J, Luo T, Wu Y, *et al*: Fabrication of Tbeta4-exosome-releasing artificial stem cells for myocardial infarction therapy by improving coronary collateralization. Bioact Mater 14: 416-429, 2022.
29. Schneider BP, Winer EP, Foulkes WD, Garber J, Perou CM, Richardson A, Sledge GW and Carey LA: Triple-negative breast cancer: Risk factors to potential targets. Clin Cancer Res 14: 8010-8018, 2008.
30. Yang P, Li J, Peng C, Tan Y, Chen R, Peng W, Gu Q, Zhou J, Wang L, Tang J, *et al*: TCONS_00012883 promotes proliferation and metastasis via DDX3/YY1/MMP1/PI3K-AKT axis in colorectal cancer. Clin Transl Med 10: e211, 2020.
31. Yu J, Wang F, Zhang J, Li J, Chen X and Han G: LINC00667/miR-449b-5p/YY1 axis promotes cell proliferation and migration in colorectal cancer. Cancer Cell Int 20: 322, 2020.
32. Mohamed TMA, Ang YS, Radzinsky E, Zhou P, Huang Y, Elfenbein A, Foley A, Magnitsky S and Srivastava D: Regulation of cell cycle to stimulate adult cardiomyocyte proliferation and cardiac regeneration. Cell 173: 104-116.e12, 2018.
33. Pike MC, Spicer DV, Dahmoush L and Press MF: Estrogens, progestogens, normal breast cell proliferation, and breast cancer risk. Epidemiol Rev 15: 17-35, 1993.
34. Matson JP and Cook JG: Cell cycle proliferation decisions: The impact of single cell analyses. FEBS J 284: 362-375, 2017.
35. Shostak A: Circadian clock, cell division, and cancer: From molecules to organism. Int J Mol Sci 18: 873, 2017.
36. Massague J: G1 cell-cycle control and cancer. Nature 432: 298-306, 2004.
37. Bartek J and Lukas J: Pathways governing G1/S transition and their response to DNA damage. FEBS Lett 490: 117-122, 2001.
38. Lupski JR: Genomic disorders: Structural features of the genome can lead to DNA rearrangements and human disease traits. Trends Genet 14: 417-422, 1998.
39. Mizuno K, Miyabe I, Schalbetter SA, Carr AM and Murray JM: Recombination-restarted replication makes inverted chromosome fusions at inverted repeats. Nature 493: 246-249, 2013.
40. Nowosad A and Besson A: Lysosomes at the crossroads of cell metabolism, cell cycle, and stemness. Int J Mol Sci 23: 2290, 2022.
41. Umeda S, Kanda M, Shimizu D, Nakamura S, Sawaki K, Inokawa Y, Hattori N, Hayashi M, Tanaka C, Nakayama G and Kodera Y: Lysosomal-associated membrane protein family member 5 promotes the metastatic potential of gastric cancer cells. Gastric Cancer 25: 558-572, 2022.
42. Finicle BT, Jayashankar V and Edinger AL: Nutrient scavenging in cancer. Nat Rev Cancer 18: 619-633, 2018.
43. Kang HJ, Jung SK, Kim SJ and Chung SJ: Structure of human alpha-enolase (hENO1), a multifunctional glycolytic enzyme. Acta Crystallogr D Biol Crystallogr 64: 651-657, 2008.
44. Cappello P, Principe M, Bulfamante S and Novelli F: Alpha-enolase (ENO1), a potential target in novel immunotherapies. Front Biosci (Landmark Ed) 22: 944-959, 2017.
45. Principe M, Borgoni S, Cascione M, Chattaragada MS, Ferri-Borgogno S, Capello M, Bulfamante S, Chapelle J, Modugno FD, Defilippi P, *et al*: Alpha-enolase (ENO1) controls alpha v/beta 3 integrin expression and regulates pancreatic cancer adhesion, invasion, and metastasis. J Hematol Oncol 10: 16, 2017.
46. Ji M, Wang Z, Chen J, Gu L, Chen M, Ding Y and Liu T: Up-regulated ENO1 promotes the bladder cancer cell growth and proliferation via regulating beta-catenin. Biosci Rep 39: BSR20190503, 2019.
47. Zhang J, Li H, Miao L and Ding J: Silencing of ENO1 inhibits the proliferation, migration and invasion of human breast cancer cells. J BUON 25: 696-701, 2020.

48. Song Y, Luo Q, Long H, Hu Z, Que T, Zhang X, Li Z, Wang G, Yi L, Liu Z, *et al*: Alpha-enolase as a potential cancer prognostic marker promotes cell growth, migration, and invasion in glioma. Mol Cancer 13: 65, 2014.
49. Min Y, Kim MJ, Lee S, Chun E and Lee KY: Inhibition of TRAF6 ubiquitin-ligase activity by PRDX1 leads to inhibition of NFKB activation and autophagy activation. Autophagy 14: 1347-1358, 2018.
50. Coumans JV, Gau D, Poljak A, Wasinger V, Roy P and Moens PD: Profilin-1 overexpression in MDA-MB-231 breast cancer cells is associated with alterations in proteomics biomarkers of cell proliferation, survival, and motility as revealed by global proteomics analyses. OMICS 18: 778-791, 2014.
51. Biterge-Sut B: Alterations in eukaryotic elongation factor complex proteins (EEF1s) in cancer and their implications in epigenetic regulation. Life Sci 238: 116977, 2019.
52. Palacios G, Shaw TI, Li Y, Singh RK, Valentine M, Sandlund JT, Lim MS, Mullighan CG and Leventaki V: Novel ALK fusion in anaplastic large cell lymphoma involving EEF1G, a subunit of the eukaryotic elongation factor-1 complex. Leukemia 31: 743-747, 2017.
53. Bengsch F, Tu Z, Tang HY, Zhu H, Speicher DW and Zhang R: Comprehensive analysis of the ubiquitinome during oncogene-induced senescence in human fibroblasts. Cell Cycle 14: 1540-1547, 2015.